Quantitative trait loci mapping reveals important genomic regions controlling root architecture and shoot biomass under nitrogen, phosphorus, and potassium stress in rapeseed (*Brassica napus* L.)

Nazir Ahmad[1†], Sani Ibrahim[1†], Ze Tian[1], Lieqiong Kuang[1], Xinfa Wang[1,2], Hanzhong Wang[1,2]* and Xiaoling Dun[1]*

[1]Key Laboratory of Biology and Genetic Improvement of Oil Crops, Oil Crops Research Institute of the Chinese Academy of Agricultural Sciences, Ministry of Agriculture, Wuhan, China, [2]Hubei Hongshan Laboratory, Wuhan, China

Plants rely on root systems for nutrient uptake from soils. Marker-assisted selection helps breeders to select desirable root traits for effective nutrient uptake. Here, 12 root and biomass traits were investigated at the seedling stage under low nitrogen (LN), low phosphorus (LP), and low potassium (LK) conditions, respectively, in a recombinant inbred line (RIL) population, which was generated from *Brassica napus* L. Zhongshuang11 and 4D122 with significant differences in root traits and nutrient efficiency. Significant differences for all the investigated traits were observed among RILs, with high heritabilities (0.43−0.74) and high correlations between the different treatments. Quantitative trait loci (QTL) mapping identified 57, 27, and 36 loci, explaining 4.1−10.9, 4.6−10.8, and 4.9−17.4% phenotypic variances under LN, LP, and LK, respectively. Through QTL-meta analysis, these loci were integrated into 18 significant QTL clusters. Four major QTL clusters involved 25 QTLs that could be repeatedly detected and explained more than 10% phenotypic variances, including two NPK-common and two specific QTL clusters (K and NK-specific), indicating their critical role in cooperative nutrients uptake of N, P, and K. Moreover, 264 genes within the four major QTL clusters having high expressions in roots and SNP/InDel variations between two parents were identified as potential candidate genes. Thirty-eight of them have been reported to be associated with root growth and development and/or nutrient stress tolerance. These key loci and candidate genes lay the foundation for deeper dissection of the NPK starvation response mechanisms in *B. napus*.

Introduction

In agricultural systems, nitrogen (N), phosphorus (P), and potassium (K) are the three most important minerals that limit plant growth. A considerable amount of fertilizer has been utilized to meet N, P, and K requirements to enhance crop production. As a result, improper practices have led to serious environmental issues, low fertilizer utilization efficiency, and excessive annual energy usage (Jiao et al., 2016). For example, globally, P resources are expected to be depleted by the end of the century (Mensah et al., 2020). Therefore, it is critical to breed crop varieties that efficiently use nutrients (mainly N, P, and K) (Stahl et al., 2019). These new cultivars should provide a more cost-effective approach than relying solely on fertilizer application (Tian et al., 2016).

Roots are responsible for water absorption, nutrient uptake, and anchoring the plant in the soil and thus substantially impact crop growth and yield formation (Atkinson et al., 2019; Chen et al., 2020). Root growth regulation has been the subject of extensive research and practice to boost grain yields (Thorup-Kristensen and Kirkegaard, 2016; Calleja-Cabrera et al., 2020). Enhancing root absorption and uptake of nutrients and water is encouraged to increase agricultural output and nutrient and water usage efficiency and minimize groundwater pollution (Hatfield and Dold, 2019). Plant root systems are dynamic structures that influence overall architecture by changing root branching, root angle, and root development rates. An effective root system is critical for nutrient uptake in plants. For example, in most elite cultivars, increasing the root-to-shoot ratio facilitates the uptake of P from deep soil and promotes the growth of longer root hairs to better utilize soil spatial features in order to store nutrients in shoots (Guo and Xu, 2012; Wang et al., 2019). Therefore, optimizing root and biomass-related traits such as root length, root width, root tips, root diameter, root, and shoot biomass at the seedling stage may thus provide a feasible route for understanding early variations linked with high nutrient-uptake. Moreover, it has been determined that genetic diversity of root-related traits is necessary to increase grain yield under different nutritional conditions (Carvalho et al., 2014; Liu et al., 2017). Hence, improving nutrient uptake through useful variation in seedling root and biomass traits under different growth conditions may be a sustainable long-term strategy for developing superior cultivars (Lynch, 2019).

An effective strategy for enhancing yield production under abiotic stress conditions requires genetic assessment of quantitative traits that determine crop adaptation to adverse conditions (Li et al., 2014). It is important to note that crop performance is the consequence of thousands of gene interactions, as well as environmental and cultural practices (Collins, 2008); it is obvious that assessing quantitative trait loci (QTLs) is a powerful tool for dissecting complex quantitative traits that have been widely studied in various crops such as in wheat (Ren et al., 2017), rice (Jewel et al., 2019), maize (Sun et al., 2021), and rapeseed (Wang et al., 2017; Dun et al., 2019; Ibrahim et al., 2021; Li et al., 2021). As QTLs were identified to be linked with phenotypic variance, the corresponding loci may be amplified and thus could be used for phenotypic improvement (Liu et al., 2021; Ma et al., 2021; Peltier et al., 2021). Understanding the genetic basis for nutrient acquisition related to root development is crucial in plant breeding (Wissuwa et al., 2016). Although extensive advances have been made in understanding how plants respond to nutrition stress, many genetic bases for nutrient tolerance remain still unclear in rapeseed (Congreves et al., 2021). Only a few studies have been conducted on QTLs that allow plants to adapt to varying N, P, and K levels under uniform conditions (Guo and Xu, 2012; Wang et al., 2012a; Shen et al., 2019).

Rapeseed (*Brassica napus* L.), a globally grown *Brassica* genus crop, is an essential vegetable oil source that humans have consumed. Understanding the molecular processes influencing root development is critical for evaluating root system architecture (RSA), nutrient efficiency, and rapeseed yield potential (McGrail et al., 2020). A panel of 236 rapeseed recombinant inbred lines (RILs) was used in this study to explore root and biomass-related traits of seedling plants in hydroponics under low Nitrogen (LN), low phosphorous (LP), and low potassium (LK) conditions. The study's ultimate objectives were as follows to (i) ascertain QTLs for root and biomass-related traits under LN, LP, and LK conditions (ii) detect major QTL clusters and determine their consistency across environments and different NPK nutritional routines to locate places with breeding prospects (iii) determine sequence variation in the crucial candidate genes (iv) find crucial candidate genes in the major QTL clusters.

Materials and methods

Plant materials

A cross of "Zhongshuang 11 (ZS11)" and "4D122" generated the RIL population ($F_{2:6}$) generation used in this experiment. The F_1 generation plants were self-pollinated to obtain F_2 generation seeds, and the F_2 generation was continuously selfed by the single seed descent method. $F_{2:6}$ seeds were obtained as the recombined inbred line population, and 236 lines were randomly selected from the ($F_{2:6}$) generation and used for this experiment (Kuang et al., 2022). The two parents were used for the pilot experiment first to find the suitable concentration of nitrogen, phosphorus and potassium, the results of which were used for low-NPK treatment for screening the RIL population.

Experimental design and hydroponic culture condition

The two parents were grown hydroponically and analyzed in two independent trials with a completely random design at the Chinese Academy of Agricultural Sciences' Oil Crops Research Institute in Wuhan, China. The seeds germinated in the greenhouse for 6 days, with 2 days of darkness and 4 days of light, before being transplanted into smaller blue plastic basins (34 cm × 26 cm × 12 cm) with a quarter-strength nutritional solution. A standard Hoagland's solution (Hoagland and Arnon, 1950), with consistent concentrations of other elements, and seven nitrogen, eight phosphorus, nine potassium concentrations were used, including 15, 3.5, 1.0, 0.75, 0.5, 0.375, 0.3 mMN$^+$, 1, 0.1, 0.05, 0.025, 0.01, 0.007, 0.005, 0.003 mMP$^+$ and 6, 0.6, 0.3, 0.15, 0.075, 0.05, 0.025, 0.01, and 0.005 mMK$^+$, respectively. The full-strength modified Hoagland's solution contained 5 mmol L^{-1} Ca (NO$_3$)$_2$.4H$_2$O, 5 mmol L^{-1} KNO$_3$, 2 mmol L^{-1} MgSO$_4$.7H$_2$O, 1 mmol L^{-1} KH$_2$PO$_4$, 0.05 μM EDTA-Fe, 46 μM H$_3$BO$_3$, 14 μM MnCl$_2$.4H$_2$O, 0.77 μM ZnSO$_4$.7H$_2$O, 0.32 μM CuSO$_4$, and 0.44 μM Na$_2$MoO4.2H$_2$O. Quarter strength, half strength, and full-strength nutritional solutions were utilized in that order for the first, second, and third weeks. Weekly, the nutrient solution was changed. Seedlings were grown under a 16/8 h light-dark cycle, a daily light intensity of 180 μmol photons m^{-2} s^{-1}, a day and night temperature of 26/21°C, and relative air humidity of 50–70%.

The nutrient stress of 236 "ZS11/4D122" RILs was then evaluated in the hydroponic culture at three-macronutrient stress concentrations, low N with 0.5 mM N, low P with 0.01 mM P, and low K with 0.001 mM K, respectively, under the same concentration of other elements. Three trials were repeated three times for each stress (LN1, LN2, LN3, LP1, LP2, LP3, LK1, LK2, and LK3). Six seedlings were grown for each genotype, and the nutrient solution was changed regularly as descried for pilot experiment.

Trait measurements

Three individual plants from each genotype were collected to conduct phenotypic identification, and each plant was divided into root and shoot sections. Five root morphology traits (RMT) viz. total root length (TRL), total root surface area (TSA), total root volume (TRV), total number of roots (TNR) were captured through images using a scanner (EPSON V700, Japan) and further analyzed by WinRHIZO software (Pro 2012b, Canada), while primary root length (PRL) was measured manually using a ruler. Seven biomass traits (BT), including root fresh weight (RFW), shoot fresh weight (SFW), were measured manually using a weighing balance. Root dry weight (RDW) and shoot dry weight (SDW) was measured after oven drying at 80°C until a constant weight was reached. Total dry weight (TDW) and total fresh weight (TFW) were estimated as SDW + RDW and SFW + RFW, respectively. The root to shoot fresh weight ratio (RSR) was calculated as the ratio between RFW and SFW.

Phenotypic data analysis and quantitative trait loci mapping

For phenotypic and QTL analysis, all 12 investigated traits were represented by the best linear unbiased estimation (BLUE) value of three plants per genotype under NPK-stress only since the results of QTL mapping under normal conditions were shown in the previous study (Kuang et al., 2022). The "*PerformanceAnalytics*" package in R software was used to calculate Pearson correlation at a significance level of $P < 0.05$. For all traits under stress treatments, analysis of variance (ANOVA) and broad-sense heritability (h^2) were performed with QRL IciMapping 4.1[1] with the ANOVA function. A total of three phenotypic datasets (LN-BLUE, LP-BLUE, and LK-BLUE) of each trial were used to map QTLs based on the construction of a genetic linkage map of the RIL population using a *Brassica 50K SNP Chip* (Kuang et al., 2022). QTL mapping was performed with the help of the software Windows QTL Cartographer 2.5, using the composite interval mapping (CIM) approach (Wang et al., 2012b). A permutation test was performed 1,000 times with a walking speed of 1 cM at a significance level of $P < 0.05$ to reduce the type-I experimental error rate (Churchill and Doerge, 1994).

The approach suggested by Wang et al. (2016) was used for QTL integration and nomenclature. To distinguish loci identified under LN from those identified under LP and LK, "LN" was added to the QTL name. Stoll et al. (2000) defined a QTL cluster as the two markers that are closest to each other and have an overlapping confidence interval (CI). Accordingly, a QTL cluster was defined as two or more significant QTLs with overlapping CI, expressed as a map distance (LOD ≥ 2.5), and labeled "qc."

Mining of candidate genes and protein interaction analysis for major quantitative trait loci clusters

In accordance with Cai et al. (2015), candidate genes were identified. All SNPs in the genetic map were used to confirm the alignment of the physical and genetic maps. Illumina Inc. created 50 K probe sequences to locate homologous loci using the NCBI local blastn program against the *Darmor-bzh* reference genome for *B. napus* (Rotmistrovsky et al., 2004; Chao et al., 2017). QTL regions were defined as genomic regions aligned with QTL's confidence interval, and genes

---

1 https://isbreedingen.caas.cn/software/qtllcimapping/294607.htm

found within the QTL were classified as candidate genes for the QTL (Chao et al., 2017). SNP/insertion-deletion (InDel) variants of potential genes were examined using the two parents' re-sequencing data (PRJNA868428). To explore the functional interactions between the genes, we used the STRING database[2] to build a protein interaction network using 264 potential candidate genes. We used the Arabidopsis thaliana homologous genes to find protein-protein interaction network.
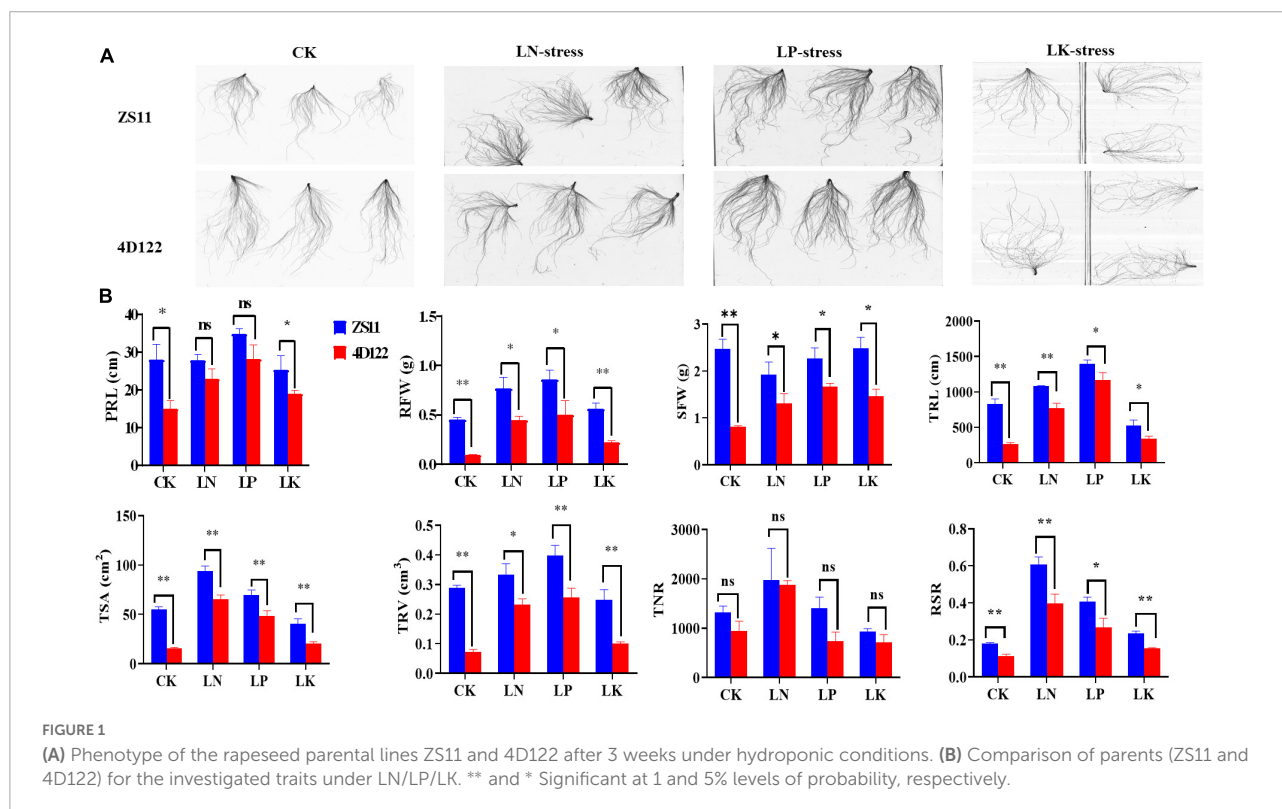
Results

Phenotypic variations of investigated traits under NPK stress conditions

A total of 12 traits, five root morphology traits (RMT) viz. PRL, TRL, TSA, TRV, TNR, and seven biomass traits (BT), RFW, SFW, RDW, SDW, TDW, TFW, and RSR, were investigated for both the parents and RIL population planted in three hydroponics trails under LN, LP, and LK treatments, respectively. Parents "ZS11 and 4D122" exhibited obvious phenotypic differences under CK/LN/LP/LK conditions (Figure 1A). The parent Zhongshuang11 (ZS11), showed

_____
2   https://string-db.org/cgi/

significant advantages for most of the investigated traits under either CK or NPK treatment over that of another parent, 4D122 (Figure 1B). These extensive genetic variations between the two parents indicated different genetic effects on the studied traits.

ANOVA revealed that genotypes, treatments, and genotype × treatment interactions significantly affected nine traits (PRL, RFW, SFW, TRL, TSA, TRV, TNR, RSR, and TFW) (Supplementary Table 1). The phenotypic performance and broad-sense heritability (h^2) for the examined traits in the RIL population are displayed (Table 1). Among the RIL population, higher and lower values than those in two parents were found under NPK-stress, implying the possibility of transgressive variation and the presence of negative and positive alleles in both parents (Table 1). The estimated h^2 for the studied traits under LN/LP/LK ranged from 0.55 to 0.74, 0.43–0.73, and 0.47–0.70, respectively. High h^2 values indicated that the genetic analysis of investigated traits in this study was reliable and suitable for QTL mapping. The coefficients of variation (CV) for different root and biomass traits under LN/LP/LK ranged from 10.9–21.3, 9.6–39.1, and 12.4–34.7%, respectively. The absolute skewness and kurtosis values for some of the investigated traits were less than 1.0 (Table 1 and Supplementary Table 2). All the studied traits exhibited normal or skewed normal distribution under LN/LP/LK (Figure 2A). These suggested that multiple genes controlled the corresponding traits.

FIGURE 1
(A) Phenotype of the rapeseed parental lines ZS11 and 4D122 after 3 weeks under hydroponic conditions. **(B)** Comparison of parents (ZS11 and 4D122) for the investigated traits under LN/LP/LK. ** and * Significant at 1 and 5% levels of probability, respectively.

Correlation analysis among the investigated traits

Significant and strong correlations were observed among the investigated traits under LN/LP/LK conditions (Figure 2A). Consistent with the correlations under the control condition (Kuang et al., 2022), RFW revealed significant and positive correlations with the other six BT, SFW (r = 0.66, 0.62, and 0.65, P < 0.01), SDW (r = 0.64, 0.50, 0.55, P < 0.01), RDW (r = 0.74, 0.76, 0.45, P < 0.01), TDW (r = 0.67, 0.59, 0.68, P < 0.01), and TFW (r = 0.75, 0.78, 0.75, P < 0.01), as well
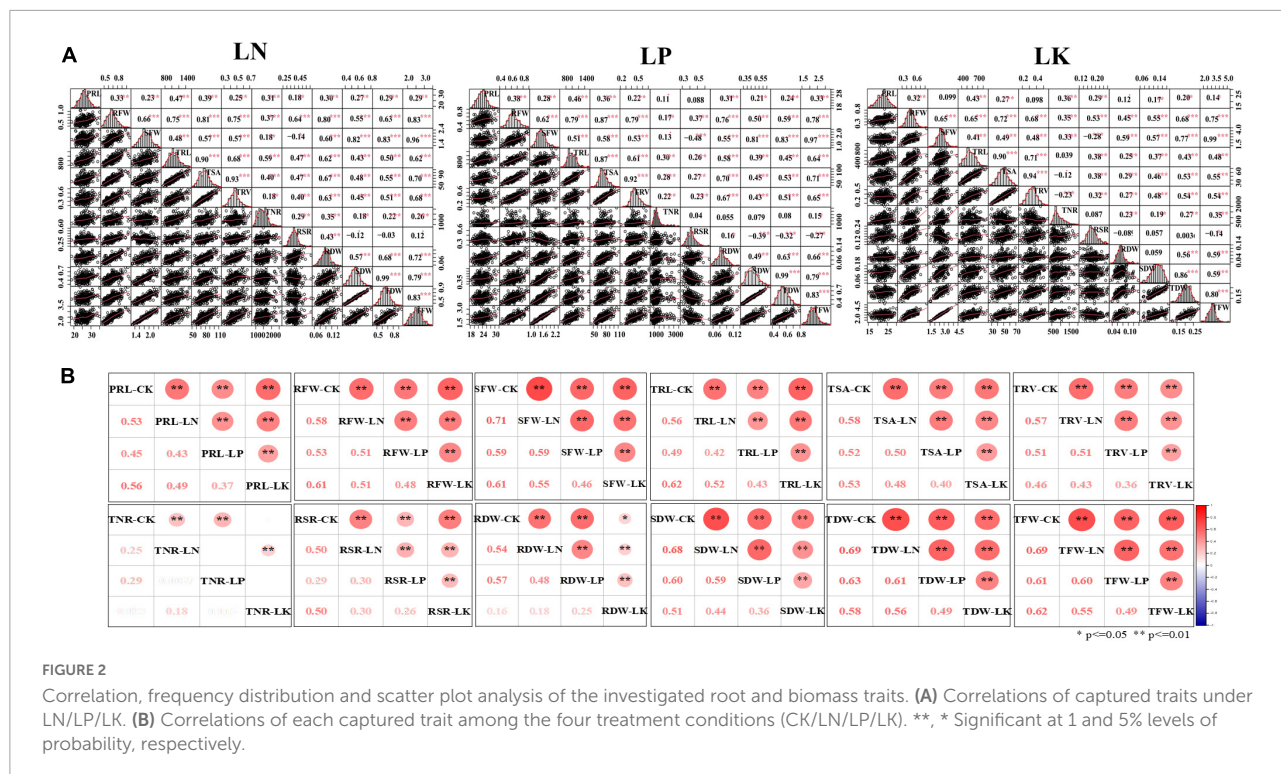
as the four RMT, TRL (r = 0.60, 0.79 and 0.65, P < 0.01), TSA (r = 0.73, 0.87, 0.72, P < 0.01), TRV (r = 0.72, 0.79, 0.68., P < 0.01), TNR (r = 0.37, 0.17, 0.35, P < 0.01), under LN/LP/LK conditions, respectively. SFW also displayed positive and significant correlation with the four RMT, TRL (r = 0.30, 0.51, 0.41, P < 0.01), TSA (r = 0.44, 0.58, 0.49, P < 0.01), TRV (r = 0.50, 0.53, 0.48, P < 0.01), TNR (r = 0.28, 0.13, 0.33, P < 0.01). Other root and biomass traits also revealed a significant and positive correlation with each other. RSR showed significant and negative correlations with SFW, SDW, TFW, and TDW. In addition, under four different treatment conditions,

TABLE 1 Descriptive statistics for investigated traits under NPK-stress in the recombinant inbred line (RIL) population.

Traits	Treat[a]	Mean	Min[b]	Max[c]	SD[d]	CV[e] (%)	Skewness	Kurtosis	[f]h^2
PRL (cm)	LN	26.2	18.7	35.1	2.85	10.9	0.33	0.23	0.58
	LP	23.8	18.2	31.7	2.28	9.6	0.34	0.52	0.49
	LK	22.6	15.0	29.9	2.81	12.4	−0.11	−0.18	0.61
RFW (g)	LN	0.687	0.451	1.074	0.11	16.2	0.56	0.55	0.70
	LP	0.629	0.418	0.893	0.09	14.2	0.43	0.41	0.61
	LK	0.474	0.268	0.835	0.08	17.6	0.38	0.97	0.70
SFW (g)	LN	1.827	1.284	2.464	0.23	12.8	0.06	−0.30	0.73
	LP	1.574	1.027	2.420	0.24	15.2	0.60	0.77	0.73
	LK	2.607	1.363	4.388	0.40	15.4	0.36	1.53	0.62
TRL (cm)	LN	1061.6	719.6	1536.0	154.60	14.6	0.56	0.21	0.65
	LP	976.3	639.0	1530.7	138.34	14.2	0.74	1.44	0.60
	LK	568.2	357.8	874.0	93.85	16.5	0.26	−0.01	0.56
TSA (cm^2)	LN	77.7	51.0	113.7	11.17	14.4	0.40	0.16	0.63
	LP	73.1	44.4	111.9	10.58	14.5	0.64	0.71	0.58
	LK	49.2	28.6	72.5	8.42	17.1	0.08	−0.15	0.49
TRV (cm^3)	LN	0.465	0.279	0.713	0.08	16.8	0.32	0.24	0.59
	LP	0.448	0.213	0.711	0.08	18.1	0.54	0.36	0.58
	LK	0.349	0.166	0.558	0.07	20.4	0.15	−0.10	0.47
TNR	LN	1471	816	2601	313.40	21.3	0.65	0.58	0.55
	LP	1295	688	3549	506.60	39.1	2.16	5.10	0.43
	LK	850	390	1996	295.20	34.7	1.15	1.20	0.52
RSR	LN	0.389	0.251	0.611	0.05	12.4	0.53	1.85	0.62
	LP	0.415	0.287	0.657	0.05	13.2	0.68	1.29	0.58
	LK	0.185	0.124	0.262	0.03	14.3	0.48	0.45	0.68
TFW (g)	LN	2.514	1.773	3.442	0.32	12.7	0.11	−0.26	0.74
	LP	2.202	1.490	3.288	0.30	13.7	0.57	0.95	0.72
	LK	3.081	1.700	5.224	0.46	14.9	0.34	1.86	0.63
RDW (g)	LN	0.100	0.056	0.153	0.02	15.8	0.20	0.45	–
	LP	0.086	0.055	0.138	0.01	16.1	0.40	0.48	–
	LK	0.071	0.033	0.138	0.02	21.1	1.10	2.73	–
SDW (g)	LN	0.556	0.372	0.807	0.08	14.3	0.23	0.24	–
	LP	0.456	0.328	0.683	0.07	14.7	0.48	0.06	–
	LK	0.136	0.073	0.188	0.02	17.6	−0.26	−0.37	–
TDW (g)	LN	0.656	0.442	0.951	0.09	13.7	0.23	0.31	–
	LP	0.542	0.387	0.794	0.07	13.8	0.44	0.18	–
	LK	0.208	0.113	0.283	0.03	14.0	−0.24	0.05	–

[a]Treat, treatment; [b]Min, minimum; [c]Max, maximum; [d]SD, standard deviation; [e]CV, coefficient of variation; [f]h^2, heritability.

FIGURE 2
Correlation, frequency distribution and scatter plot analysis of the investigated root and biomass traits. **(A)** Correlations of captured traits under LN/LP/LK. **(B)** Correlations of each captured trait among the four treatment conditions (CK/LN/LP/LK). **, * Significant at 1 and 5% levels of probability, respectively.

CK/LN/LP/LK, significant and positive correlations were found among the studied traits (Figure 2B). For examples, correlation coefficients for PRL ranged from 0.37 to 0.56, RFW (0.48–0.61), SFW (0.46–0.71), TRL (0.42–0.62), TSA (0.40–0.58), TRV (0.36–0.57), RSR (0.26–0.50), RDW (0.16–0.57), SDW (0.36–0.68), TDW (0.49–0.69), and TFW (0.49–0.69). TNR showed a weak correlation (0.18–0.25) under different treatments. These results indicated the genetic stability of these traits across different stress conditions. Moreover, high correlations proves common genetic factors controlling the studied traits under all of the CK, LN, LP, and LK treatments.

Quantitative trait loci mapping

Quantitative trait loci detected for root and biomass traits under low nitrogen-stress condition

Using a high-density SNP linkage mapping, a total of 57 loci associated with 12 root and biomass traits, were detected on 15 linkage groups (A01: 2, A02: 2, A03: 1, A04: 1, A05: 2, A08: 11, A09: 9, A10: 5, C01: 6, C02: 5, C03: 1, C04: 3, C06: 2, C07: 1, and C08: 6) under the LN condition in this RIL population, explaining 4.1–10.9% phenotypic variance (R^2) (Figure 3A and Supplementary Table 3). Among these, 20 loci for RMT (including "PRL: 8, TRL: 3, TSA: 3, TRV: 4, and TNR: 2") and 37 loci for BT ("RFW: 8, SFW: 10, RSR: 1, RDW: 4, SDW: 6, and TDW: 8") were observed under the LN condition.

High phenotypic variance (PVE) were explained by these loci for RMT and BT ("PRL: 50.6%, TRL: 18.8%, TSA: 17.9%, TRV: 30.9%, TNR: 13.1%, RFW: 45.6%, SFW: 69.9%, RDW: 23.6%, SDW: 39.1%, TDW: 54.6%, and RSR: 7.2%"). 53% (30 loci), and 47% (27 loci) were identified with positive and negative additive effects, indicating the importance of both parents toward the investigated traits.

Quantitative trait loci detected for root and biomass traits under low phosphorous-stress condition

A total of 27 loci were detected on seven linkage groups (A05: 1, A07: 1, A08: 4, A09: 10, C02: 8, C03: 1, and C08: 2), explaining 4.6–10.8% phenotypic variation under the LP condition (Figure 3B and Supplementary Table 4). These loci explained high PVE for different RMT and BT; i.e., PRL: 15.1%, TRL: 6.0%, RFW: 5.1%, SFW: 33.3%, RDW: 4.9%, SDW: 61.5%, TDW: 59.6%, and RSR: 5.1%. Among these, three loci for RMT ("PRL: 2, TRL: 1) and 24 loci for BT (RFW: 1, SFW: 5, RSR: 1, RDW: 1, SDW: 8, and TDW: 8"). Maximum loci (63%, 17 loci) showed a negative additive effect, indicating the contribution of parent ZS11 toward these traits.

Quantitative trait loci detected for root and biomass traits under low potassium-stress condition

A total of 36 loci on 10 linkage groups (A01: 3, A02: 2, A07: 8, A09: 9, C01: 4, C02: 1, C03: 1, C06: 3, C07: 3, and C08: 2)
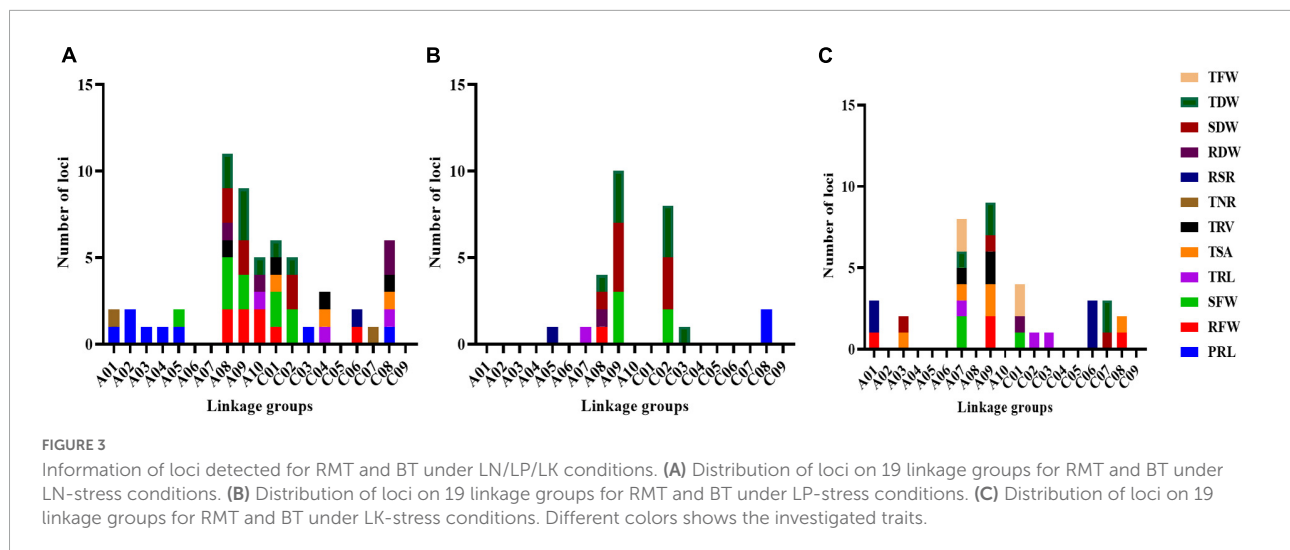
FIGURE 3
Information of loci detected for RMT and BT under LN/LP/LK conditions. **(A)** Distribution of loci on 19 linkage groups for RMT and BT under LN-stress conditions. **(B)** Distribution of loci on 19 linkage groups for RMT and BT under LP-stress conditions. **(C)** Distribution of loci on 19 linkage groups for RMT and BT under LK-stress conditions. Different colors shows the investigated traits.

were detected under the LK-stress condition (**Figure 3C** and **Supplementary Table 5**). These detected loci explained 4.9–17.4% of the total phenotypic variation. These 36 loci explained high phenotypic variance for the investigated RMT and BT (TRL: 15.9%, TSA: 35.2%, TRV: 19.5%, RFW: 22.8%, SFW: 20.7%, RDW: 6.0%, SDW: 17.9%, TDW: 32.7%, TFW: 24.1%, and RSR: 57.0%). Among 36 loci under LK-stress condition, 11 loci for RMT ("TRL: 3, TSA: 5, and TRV: 3"), while 25 loci for BT ("RFW: 4, SFW: 3, RSR: 5, RDW: 1, SDW: 3, TDW: 5, and TFW: 4) were detected. Most detected loci showed negative effects (75%, 27 loci), consistent with those under LN and LP conditions.

Identification of specific and common quantitative trait loci clusters under NPK-stress

The genomic region associated with many traits is biologically intriguing because it may harbor important regulators. It signifies the existence of a single gene with a pleiotropic effect or closely linked loci controlling two or more traits (Goto et al., 2021). The shared genomic region in this study is referred to as the QTL hotspot or QTL cluster. Based on the overlapping confidence intervals, 97 out of 120 loci were integrated through QTL-meta analysis into 18 unique pleiotropic QTL clusters under NPK-stress conditions (**Table 2, Figure 4**, and **Supplementary Table 6**). These QTL clusters explained 4.6–12.8% of the total phenotypic variance. Genetic regions of these QTL clusters were detected on 12 linkage groups; A01, A07–A10, C01–04, and C06–C08. Out of 18 QTL clusters, 12 QTL clusters exhibited a negative additive effect, indicating the significant contribution of ZS11 toward the investigated traits. We then divided the detected QTL clusters into common and specific clusters (Kim et al., 2021). Based on this, we detected two NPK-common clusters, three K-specific clusters, four N-specific clusters, four PK-specific clusters, three NK-specific clusters, and two NP-specific clusters (**Table 2** and

Figure 4), suggesting that key loci associated with these traits under multiple environments or treatments.

Quantitative trait loci clusters that explain more than 10% of phenotypic variance (R^2) and could be repeatedly detected under different environments or repetitions are referred to as major QTL clusters. Consequently, we detected four major QTL clusters associated with NPK-stress (**Table 3** and **Figure 4**). Two NPK-common and two specific QTL clusters (K and NK-specific) were found among the identified major QTL clusters. Further, these QTL clusters may be used to predict candidate genes and conduct marker-assisted selection (MAS).

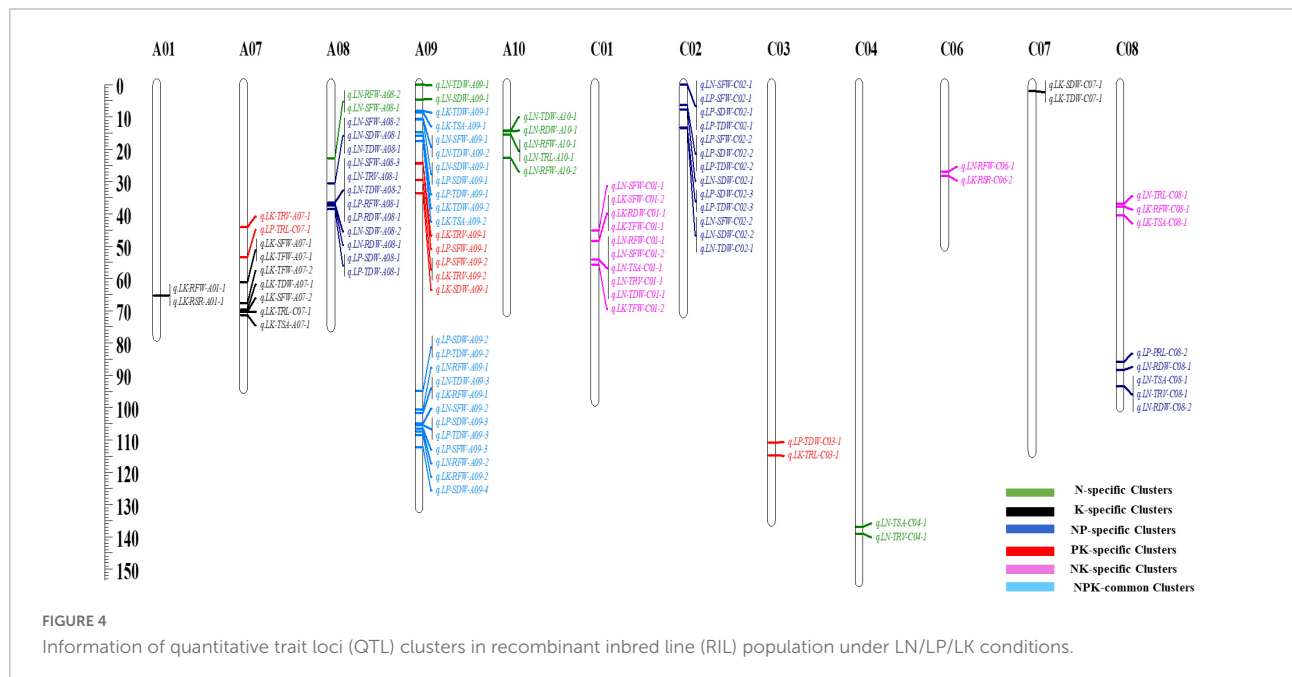## Candidate gene prediction and protein interaction analysis in the major quantitative trait loci clusters

All the annotated genes within the four major QTL clusters were retrieved according to the genome sequence of *Darmor*. As a result, 1,655 annotated gene models were found, with a gene number ranging from 168 to 631 in each major QTL cluster (**Supplementary Table 7**). Based on the annotation data of the retrieved genes as well as functions defined for their homologs in *A. thaliana*, the corresponding gene function was predicted (**Supplementary Table 7**). Furthermore, the corresponding gene information of the 1655 annotated genes in the ZS11 genome were checked. Among these, genes having high expressions in roots using the BnTIR database[3] and having SNPs (missense variant) or indels effect (disruptive inframe deletion/insertion) between the two parents using the re-sequence data of 4D122 and the deno-genome sequence of ZS11 were selected. As a result, we found 264 potential candidate genes (**Supplementary Tables 8–10**) that were capable of fulfilling these two criteria. Among these, some were also found to be highly expressed

---

3   http://yanglab.hzau.edu.cn/BnTIR

TABLE 2 Summary of quantitative trait loci (QTL) clusters detected under NPK-stress in the recombinant inbred line (RIL) population.

QTL clusters	Type	Chr.	Traits	Treatment	Peak position (cM)	C.I[a]	Max LOD	Max R^2 (%)[b]	Add[c]
qc.A01-1	K-specific	A01	RFW, RSR	LK-BLUE	65.21	61.9–67.7	8.9	12.8	(−)
qc.A07-1	PK-specific	A07	TRV, TRL	LK/LP-BLUE	53.41	37.0–56.2	3.8	6	(−)
qc.A07-2	K-specific	A07	SFW, TFW, TDW, TRL, TSA	LK-BLUE	71.31	59.6–81.4	6.2	9.2	(−)
qc.A08-1	N-specific	A08	RFW, SFW	LN-BLUE	22.81	17.3–24.6	4.6	6.3	(−)
qc.A08-2	NP-specific	A08	SFW, SDW, TDW, TRV, RFW, RDW	LN/LP-BLUE	38.61	24.9–40.5	7.2	9.4	(−)
qc.A09-1	N-specific	A09	TDW, SDW	LN-BLUE	4.51	0.0–8.1	5.2	7.3	(−)
qc.A09-2	NPK-common	A09	TDW, TSA, SFW, SDW	LN/LP//LK-BLUE	17.41	6.2–20.7	7.8	10.9	(−)
qc.A09-3	PK-specific	A09	TRV, SFW, SDW	LP/LK-BLUE	33.51	21.6–37.0	4.9	7.0	(−)
qc.A09-4	NPK-common	A09	SDW, TDW, RFW, SFW	LN/LP//LK-BLUE	112.21	89.2–117.0	8.2	10.9	(−)
qc.A10-1	N-specific	A10	TDW, RDW, RFW, TRL	LN-BLUE	22.71	11.5–26.5	4.2	6.5	(+)
qc.C01-1	NK-specific	C01	SFW, RDW, TFW, RFW, TSA, TRV, TDW	LN/LK-BLUE	55.61	44.8–60.0	5.3	7.3	(+)
qc.C02-1	PK-specific	C02	SFW, SDW, TDW	LP/LK-BLUE	13.41	0.0–16.6	6.2	8.5	(+)
qc.C03-1	PK-specific	C03	TDW, TRL	LP/LK-BLUE	114.71	101.1–127.7	3.6	5.0	(−)
qc.C04-1	N-specific	C04	TSA, TRV	LN-BLUE	139.01	135.9–144.7	5.8	8.0	(−)
qc.C06-1	NK-specific	C06	RFW, RSR	LN/LK-BLUE	28.21	24.7–30.9	8.6	11.9	(+)
qc.C07-1	K-specific	C07	SDW, TDW	LK-BLUE	2.01	0.0–4.2	5.0	7.6	(−)
qc.C08-1	NK-specific	C08	TRL, RFW, TSA	LK-BLUE	40.41	34.0–44.0	3.7	5.4	(+)
qc.C08-2	NP-specific	C08	PRL, RDW, TSA, TRV	LN/LP-BLUE	93.31	83.0–98.3	5.1	7.7	(+)

[a]C.I, confidence interval; [b]R^2, phenotypic variance; [c]Add, additive gene effect.

FIGURE 4
Information of quantitative trait loci (QTL) clusters in recombinant inbred line (RIL) population under LN/LP/LK conditions.

in the root, stem, cotyledon, silique, silique wall, leaf, seed, and bud, implying that they are involved in plant growth and development (Figure 5A).
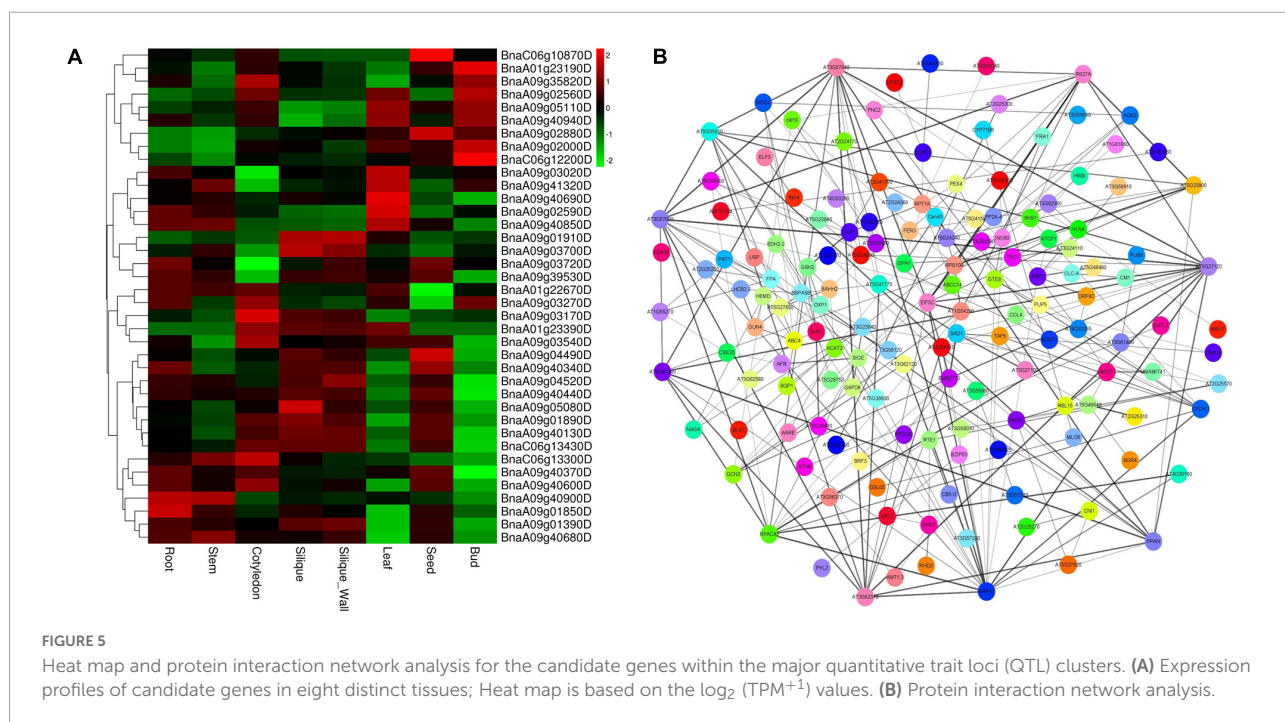
In living organisms, protein–protein interactions (PPIs) play a role in almost all biological processes (Rao et al., 2014); therefore, a protein interaction analysis was performed using the STRING database (Szklarczyk et al., 2021) (see footnote 2) to explore the candidate genes' functional interactions further. Out of 264 potential candidate genes, the Arabidopsis orthologs of 262 were found that exhibit strong protein interaction with

TABLE 3 Information of major quantitative trait loci (QTL) clusters with their physical position detected under NPK-stress in the recombinant inbred line (RIL) population.

Major QTL clusters	Type	Chr.	Traits	Treat	Peak position-cM (Mb)	C.I[a]	Physical position (Mb)	Max LOD	Max[b] R^2(%)	Add[c]
qc.A01-1	K-specific	A01	RFW, RSR	LK-BLUE	65.21 (15.59)	61.9–67.7	14.63–16.41	8.9	12.8	(−)
qc.A09-2	NPK-common	A09	TDW, TSA, SFW, SDW	LN/LP//LK-BLUE	17.41 (2.52)	6.2–20.7	0.73–3.02	7.8	10.9	(−)
qc.A09-4	NPK-common	A09	SDW, TDW, RFW, SFW	LN/LP//LK-BLUE	112.21 (28.42)	89.2–117.0	25.77–29.06	8.2	10.9	(−)
qc.C06-1	NK-specific	C06	RFW, RSR	LN/LK-BLUE	28.21 (14.64)	24.7–30.9	12.04–16.69	8.6	11.9	(+)

FIGURE 5
Heat map and protein interaction network analysis for the candidate genes within the major quantitative trait loci (QTL) clusters. (A) Expression profiles of candidate genes in eight distinct tissues; Heat map is based on the log$_2$ (TPM^{+1}) values. (B) Protein interaction network analysis.

each other (**Supplementary Table 10** and **Figure 5B**). According to previous studies, we found 38 out of 264 candidate genes, three from *qcA01-1*, 18 from *qcA09-2*, 13 and 4 from *qcA09-4,* and *qcC06-1,* known to be involved in root growth and development or nutrient utilization (**Table 4**). According to the protein interaction network analysis, the predicted genes were strongly interconnected and may play a major role in *NPK* stress tolerance through their interactions with other associated genes. These findings imply that these genes should be explored in greater detail to better understand their putative functions in the protein interaction network.

Discussion

Correlation studies help breeders in identifying the fundamental traits for which selection can be based on population improvement (Jewel et al., 2019). Significant and

strong positive correlations were observed among most of the studied traits under NPK-stress conditions (**Figure 2A**). At the same time, RSR exhibited a significant negative correlation with SFW, SDW, TDW, and TFW stress conditions. Here, we want to highlight that RSR may be a key phenotypic trait due to its sensitivity to nutritional stress; these findings are congruent with those for rapeseed (Dun et al., 2019). Highly correlated traits with a shared genetic basis were identified, demonstrating that these 12 root and biomass traits could be used to assess NPK-deficiency tolerance in RILs at the seedling stage (Liu et al., 2017). Heritability for RDW, SDW, and TDW has not been included because these dry weights were measured as sum of three plants. Root and biomass traits had significant heritabilities and genetic variations, suggesting that they might be used as primary selection criteria for optimizing nutrient use efficiency and uncovering underlying genetics (Hawkesford and Griffiths, 2019; Jewel et al., 2019). These findings confirmed prior studies by emphasizing the role of root development

TABLE 4 Important candidate genes within the major quantitative trait loci (QTL) clusters related to root development/nutrient utilization.

Gene ID in *Darmor*	QTL cluster	Distance to Peak position (Mb)	Homologs in At.	Function annotation	References
BnaA01g22670D	qc.A01-1	0.57	AT1G61660.1	PFA4, enhance stress tolerance and governs the competence of pericycle cells to initiate lateral root primordium formation	Woo et al., 2012
BnaA01g23190D	qc.A01-1	0.00	AT3G24300.1	AMT1:3, Involved in lateral root formation and branching and ammonium homeostasis	Vega et al., 2021
BnaA01g23390D	qc.A01-1	−0.18	AT3G24160.1	PMP, Encodes a putative Type 1 membrane protein	Colinas and Fitzpatrick, 2016
BnaA09g01390D	qc.A09-2	1.78	AT4G03210.1	XTH9, Plant-type secondary cell wall biogenesis	Xu and Cai, 2019
BnaA09g01850D	qc.A09-2	1.57	AT3G27000.1	ARP2, Involved in cell morphogenesis	Chin et al., 2021; García-González and van Gelderen, 2021
BnaA09g01890D	qc.A09-2	1.56	AT3G27090.1	NRP2, involved in regulation of the protein catabolic process	Wu et al., 2022
BnaA09g01910D	qc.A09-2	1.55	AT3G27160.1	GHS1, Required for photosynthesis and C/N balance	Dong and Duan, 2020
BnaA09g02000D	qc.A09-2	1.52	AT5G40650.1	SDH2-2, Involved in mitochondrial electron transport	Samuilov et al., 2018
BnaA09g02560D	qc.A09-2	1.21	AT5G39510.1	VTI11, Involved in protein trafficking to lytic vacuoles	Larson et al., 2014
BnaA09g02590D	qc.A09-2	1.19	AT3G29350.1	AHP2, Involved in cytokinin-activated signaling pathway	Justamante et al., 2019; Islam et al., 2022
BnaA09g02880D	qc.A09-2	1.06	AT5G48230.2	AAT1, Sterol metabolic process	Coleto et al., 2019
BnaA09g03020D	qc.A09-2	0.98	AT5G48430.1	NLP7, nitrate signaling	Zhao et al., 2018
BnaA09g03170D	qc.A09-2	0.92	AT5G48870.1	LSM5, response to abscisic acid and root hair growth	Marzol et al., 2022
BnaA09g03270D	qc.A09-2	0.86	AT5G49270.1	COBL9, Involved in root epidermal cell differentiation	Canales et al., 2014; Janes et al., 2018
BnaA09g03540D	qc.A09-2	0.72	AT5G29000.2	PHL1, PHL1 acts redundantly with PHR1 to regulate responses to Pi starvation.	Fan et al., 2021
BnaA09g03700D	qc.A09-2	0.67	AT5G27380.1	GHS2, Involved in glutathione synthetases	Podg et al., 2018; Trujillo-Hernandez et al., 2020
BnaA09g03720D	qc.A09-2	0.65	AT5G27420.1	ATL31, Involved in Carbon/Nitrogen response for growth phase transition	Li et al., 2020
BnaA09g04490D	qc.A09-2	0.31	AT5G25760.2	PEX4, Involved in sucrose-dependent seedling development and reduced lateral root production	Ehrary et al., 2020
BnaA09g04520D	qc.A09-2	0.29	AT5G25610.1	RD22, responsive to dehydration 22 (RD22) mediated by ABA and lateral root elongation	Lee et al., 2021
BnaA09g05080D	qc.A09-2	0.02	AT5G23950.1	Calcium-dependent lipid-binding	Bouain et al., 2019
BnaA09g05110D	qc.A09-2	0.01	AT5G23900.1	RPLD13, Ribosomal protein L13e family protein	Wang et al., 2013
BnaA09g35820D	qc.A09-4	2.34	AT3G56370.1	IRK, Inflorescence and root apices receptor kinase	Xun and Gou, 2020
BnaA09g39530D	qc.A09-4	0.40	AT3G61960.1	ATG1A, Serine/threonine-protein kinase	Bedu et al., 2020

(Continued)

TABLE 4 (Continued)

Gene ID in *Darmor*	QTL cluster	Distance to Peak position (Mb)	Homologs in At.	Function annotation	References
BnaA09g40130D	*qc.A09-4*	0.16	*AT3G62770.1*	ATG18A, Required for autophagosome formation during nutrient deprivation and senescence	Zhen et al., 2019; Huo et al., 2020
BnaA09g40340D	*qc.A09-4*	0.09	*AT3G62980.1*	TIR1, Encodes an auxin receptor that mediates auxin-regulated transcription	Yang et al., 2022
BnaA09g40370D	*qc.A09-4*	0.00	*AT3G63390.1*	Nutrients signaling	Armengaud et al., 2010
BnaA09g40440D	*qc.A09-4*	−0.04	*AT2G26540.1*	Encodes a uroporphyrinogen-III synthase involved in tetrapyrrole biosynthesis	Kuang et al., 2017
BnaA09g40600D	*qc.A09-4*	−0.11	*AT2G26300.1*	GPA1, Encodes an alpha subunit of a heterotrimeric GTP-binding protein	Sahito et al., 2020
BnaA09g40680D	*qc.A09-4*	−0.14	*AT2G26060.1*	CIA1, Encodes a homolog of the yeast Cytosolic Iron-sulfur protein	Lešková et al., 2020
BnaA09g40690D	*qc.A09-4*	−0.15	*AT2G26040.1*	PYL2, Mediate ABA-dependent regulation of protein phosphatase	Zeng et al., 2021
BnaA09g40850D	*qc.A09-4*	−0.20	*AT2G25570.3*	ISE3, SEL1-like repeat protein involved in plasmodesmata-mediated intercellular transport	Vijayakumar et al., 2016
BnaA09g40900D	*qc.A09-4*	−0.23	*AT4G32400.1*	BT1, Encodes a plastidial nucleotide uniport carrier protein required to export newly synthesized adenylates into the cytosol	Araus et al., 2016; Rossdeutsch et al., 2021
BnaA09g40940D	*qc.A09-4*	−0.24	*AT5G52560.1*	UPS, sugar pyrophosphorylase	Velinov et al., 2020
BnaA09g41320D	*qc.A09-4*	−0.48	*AT2G24540.1*	AFR, F-box protein	Rath et al., 2020
BnaC06g10870D	*qc.C06-1*	1.72	*AT5G51060.1*	RHD2, Involved in normal root hair elongation	Mase and Tsukagoshi, 2021
BnaC06g12200D	*qc.C06-1*	0.10	*AT4G30160.1*	VLN4, Encodes a major actin filament bundling protein that is involved in root hair growth	García-González and van Gelderen, 2021
BnaC06g13300D	*qc.C06-1*	−1.40	*AT5G40890.1*	CLC-A, Encodes a member of the voltage-dependent chloride channel	Alcock et al., 2018
BnaC06g13430D	*qc.C06-1*	−1.51	*AT5G41080.1*	GDPD2, Encodes a member of the glycerophosphodiester phosphodiesterase	Das et al., 2022

in improving N, P, and K efficiency under low N, P, and K conditions (Wang et al., 2017, Wang et al., 2019; Dun et al., 2019; Li et al., 2021). These kinds of variations in population for intricate root behavior may be critical for the genetic dissection of valuable loci (Danakumara et al., 2021; Sandhu et al., 2021).

Significant genetic variation among genotypes allowed researchers to investigate genetic loci linked with the observed traits (Kang et al., 2021; Roy et al., 2021). In the current study, the RIL population was phenotyped, QTL analysis was performed under LN/LP/LK treatments, and 57, 27, and 36 loci under LN, LP, and LK, respectively, that controlled nutrient deficiency were identified (Supplementary Tables 3–5). Multiple QTLs were detected for each trait, with varying contributions from both parents, revealing the possibility of epistatic interactions across both parental genomes, in which

alleles from both parents act together to express these traits. This finding supports the pyramiding of QTLs for several different traits acting same time in a specific cultivar (Dormatey et al., 2020; Mei et al., 2020). The co-localization of QTLs for many traits can be attributed to the pleiotropic effect of a single gene or a network of interrelated genes, each of which affects one trait (Amoah et al., 2020; Ibrahim et al., 2021; Prakash et al., 2021). The co-localization of 18 QTL clusters in this study suggested that this genomic region could help with breeding NPK efficiency-related root and biomass traits. Among these identified QTL clusters, seven clusters (qcA09-1, qcA09-4, qcC03-1, qcC04-1, qcC06-1, qcC08-1, and qcC08-2) have been reported recently under control condition (Kuang et al., 2022). These QTLs may be in selecting a specific or common nutrient efficiency, as direct selection for one will

result in indirect selection for the other. Furthermore, QTL clusters suggest that employing many QTLs to improve root and biomass traits is easier than using single QTLs (Hina et al., 2020). We found four major QTL clusters (two NPK-common and two K/NK-specific) that explained (R^2 > 10%) among these 18 co-localized QTL clusters, demonstrating the reliability of QTL mapping. Our study's extensive QTL cluster analysis implies that breeding programs intending to improve root and biomass traits with improved nutrient uptake efficiency should concentrate on major QTL clusters and choose loci with these regions.

Identifying potential candidate genes underlying the QTL region is extremely important for breeding programs (Wang et al., 2020; Garcia et al., 2021; Soriano et al., 2021). The sequencing and annotation of the *B. napus* genome and expression databases would contribute to the development of molecular markers and the knowledge of gene function, regulation, and expression (Lu et al., 2019). Based on gene annotations and available literature, the current experiment identified potential candidate genes influencing root and biomass traits under NPK-stress in rapeseed that underpin the four designated "QTL hotspots/major QTL clusters." Most of these potential candidate genes were significantly expressed in root and stem tissue (**Figure 5A**). Many genes orthologous to *A. thaliana* were associated with root development or nutrient utilization based on functional annotation of candidate genes. For example, *BnaA01g22670D* was located at a distance of 583 Kb from the peak position of the major QTL cluster *qcA01-1* associated with root and biomass traits under LK-stress and orthologous to *AtPFA4*, which has a potential role in phosphorus starvation in *A. thaliana* (Woo et al., 2012). Another potential candidate gene (*BnaA01g23190D, AtAMT1;3*) encoding an ammonium transporter has been reported that promotes primary and lateral root growth in response to nitrate (Vega et al., 2021).

Similarly, *BnaA01g23390D* was identified at a distance of 184 Kb from the peak position of the major QTL cluster *qcA01-1*, associated with root and biomass traits under LK-stress and orthologous to *AtPMP*, which has a crucial role in nitrogen metabolism (Colinas and Fitzpatrick, 2016). In the major QTL cluster qcA09-2, some potential candidates were also detected. For example, *BnaA09g04490D* is located at a distance of 317 Kb from the peak position of *qcA09-2* and is associated with root and biomass traits under NPK-stress. An orthologous *BnaA09g04490D* (*AtPEX4*) has been reported to regulate primary nitrate response, potentially by interfering with the *TGA1* and *TGA4* transcription factors (Ehrary et al., 2020). Another gene (*BnaA09g04520D, AtRD22*) located at 296 Kb from the peak position of major QTL cluster *qcA09-2* has been demonstrated to play a key role in nitrogen use efficiency and nitrate assimilation (Lee et al., 2021). Two important genes (*BnaA09g05080D* and *BnaA09g05110D*) located at a distance of 20 and 10 Kb from the peak position of the major QTL cluster *qcA09-2*, respectively, have been reported that play a key

role in root growth and development under phosphorus stress condition (Wang et al., 2013; Bouain et al., 2019). Several crucial candidate genes were also identified in the major QTL cluster *qcA09-4*. For example (*BnaA09g40130D*, *AtATG18A*), located at a distance of 163 Kb, has been reported to regulate nitrogen use efficiency (Zhen et al., 2019; Huo et al., 2020). Another gene (*BnaA09g40340D, AtTIR1*) found at a distance of 92 Kb from the peak position and has been reported recently that regulate root growth and thus can enhance crop production (Yang et al., 2022). *BnaA09g40370D* encoding a hypothetical protein and has been reported to regulate root growth and development in response to potassium deficiency (Armengaud et al., 2010). Another gene (*BnaA09g40440D*) located at 40 Kb upstream from the peak position of the major QTL cluster *qcA09-4* associated with root and biomass traits and has been reported that regulation nitrogen assimilation and utilization (Kuang et al., 2017). Similarly, some important candidate genes were identified in the major QTL cluster *qcC06-1*. For example, a gene (*BnaC06g12200D, AtVLN4*) has been detected at a distance of 102 Kb from the peak position and reported to regulate root growth and development under different abiotic stresses (García-González and van Gelderen, 2021). These potential candidate genes were found in strong interaction with other genes in the protein interaction network (**Figure 5B**). As discussed in **Supplementary Table 10**, these interacting genes have a potential role in root growth and development, hormone signaling pathways, and nutrient utilization. Finally, we hypothesized that the genes that were found to be orthologous to nutrient stress/tolerance genes in *A. thaliana* might be highly related to nutrient stress/tolerance in *B. napus*. Further research and validation of these genes may be carried out to confirm their role in nutrient stress/tolerance in *B. napus*. These key loci and candidate genes lay the foundation for deeper dissection of the NPK starvation response mechanisms in *B. napus*.

Conclusion

Rapeseed oil is not only widely consumed in the human diet but also the world's second-leading source of biodiesel. In many plant-breeding programs, developing crop varieties with stronger RSA is viewed as a way to reduce the use of NPK fertilizers by enhancing nutrient use efficiency and thereby increasing yield productivity. In the current study, the recombinant inbred line population originated from ZS11, the donor parent, and 4D122, the recipient parent, enabled us to uncover a large number of loci (120 QTLs) associated with root and biomass traits under NPK-deficiency. Among them, we detected 97 loci for different root and biomass traits that were integrated into 18 QTL clusters (NPK-specific and NPK-common). Four identified QTL clusters were further classified as major QTL clusters, comprised of several loci associated

with different root and biomass architectural traits under NPK-deficiency conditions. Two of these major QTL clusters were expressed in all three stress conditions, indicating an underlying uniform basis of genetic mechanisms, contributing to the tolerance of these traits. The list of detected loci and refined clusters will facilitate further validation in systematic breeding for specific adaptability under low-input conditions and suggest that the genomic regions could be used as targets to understand the RSA mechanism better and improve nutrient use efficiency in rapeseed. In the future, the detected promising harbor QTLs will lead to the fine-mapping and molecular cloning of key loci that can be used to improve grain yield and quality under low-input fertilizer management conditions.

Data availability statement

The data presented in the study are deposited in the NCBI database, https://www.ncbi.nlm.nih.gov/bioproject/PRJNA868428. The data is downloadable at this link: https://sra-download.ncbi.nlm.nih.gov/traces/sra74/SRR/020517/SRR21010126. Also accessible through this link: https://trace.ncbi.nlm.nih.gov/Traces/index.html?view=run_browser&acc=SRR21010126&display=data-access.

Author contributions

XD planned and supervised the research. NA, SI, ZT, and LK performed root traits investigation and analyzed the data. NA wrote the manuscript. XD, XW, and HW contributed to modify the manuscript. All authors contributed to the article and approved the submitted version.

Funding

Acknowledgments

Conflict of interest

The authors declare that the research was conducted in the absence of any commercial or financial relationships that could be construed as a potential conflict of interest.

Publisher's note

All claims expressed in this article are solely those of the authors and do not necessarily represent those of their affiliated organizations, or those of the publisher, the editors and the reviewers. Any product that may be evaluated in this article, or claim that may be made by its manufacturer, is not guaranteed or endorsed by the publisher.

Supplementary material

The Supplementary Material for this article can be found online at: https://www.frontiersin.org/articles/10.3389/fpls.2022.994666/full#supplementary-material

References

Alcock, T. D., Havlickova, L., He, Z., Wilson, L., Bancroft, I., White, P. J., et al. (2018). Species-wide variation in shoot nitrate concentration, and genetic loci controlling nitrate, phosphorus and potassium accumulation in *Brassica napus* L. *Front. Plant Sci.* 871:1487. doi: 10.3389/fpls.2018.01487

Amoah, N. K. A., Akromah, R., Kena, A. W., Manneh, B., Dieng, I., and Bimpong, I. K. (2020). Mapping QTLs for tolerance to salt stress at the early seedling stage in rice (*Oryza sativa* L.) using a newly identified donor 'Madina Koyo'. *Euphytica* 216:156. doi: 10.1007/s10681-020-02689-5

Araus, V., Vidal, E. A., Puelma, T., Alamos, S., Mieulet, D., Guiderdoni, E., et al. (2016). Members of BTB gene family of scaffold proteins suppress nitrate uptake and nitrogen use efficiency. *Plant Physiol.* 171, 1523–1532. doi: 10.1104/pp.15.01731

Armengaud, P., Breitling, R., and Amtmann, A. (2010). Coronatine-insensitive 1 (COI1) mediates transcriptional responses of *Arabidopsis thaliana* to external potassium supply. *Mol. Plant* 3, 390–405. doi: 10.1093/mp/ssq012

Atkinson, J. A., Pound, M. P., Bennett, M. J., and Wells, D. M. (2019). Uncovering the hidden half of plants using new advances in root phenotyping. *Curr. Opin. Biotechnol.* 55, 1–8. doi: 10.1016/j.copbio.2018.06.002

Bedu, M., Marmagne, A., Masclaux-daubresse, C., and Chardon, F. (2020). Transcriptional plasticity of autophagy-related genes correlates with the genetic response to nitrate starvation in *Arabidopsis thaliana*. *Cells* 9:1021. doi: 10.3390/cells9041021

Bouain, N., Id, A. K., Id, S. B. S., and Nam, H. (2019). Systems genomics approaches provide new insights into *Arabidopsis thaliana* root growth regulation under combinatorial mineral nutrient limitation. *PLoS Genet.* 15:e1008392. doi: 10.1371/journal.pgen.1008392

Cai, G., Yang, Q., Yi, B., Fan, C., Zhang, C., Edwards, D., et al. (2015). A bi-filtering method for processing single nucleotide polymorphism array data improves the quality of genetic map and accuracy of quantitative trait locus mapping in doubled haploid populations of polyploid *Brassica napus*. *BMC Genomics* 16:409. doi: 10.1186/s12864-015-1559-4

Calleja-Cabrera, J., Boter, M., Oñate-Sánchez, L., and Pernas, M. (2020). Root growth adaptation to climate change in crops. *Front. Plant Sci.* 11:544. doi: 10.3389/fpls.2020.00544

Canales, J., Moyano, T. C., Villarroel, E., and Gutiérrez, R. A. (2014). Systems analysis of transcriptome data provides new hypotheses about *Arabidopsis* root response to nitrate treatments. *Front. Plant Sci.* 5:22. doi: 10.3389/fpls.2014.00022

Carvalho, P., Azam-Ali, S., and Foulkes, M. J. (2014). Quantifying relationships between rooting traits and water uptake under drought in Mediterranean barley and durum wheat. *J. Integr. Plant Biol.* 56, 455–469. doi: 10.1111/jipb.12109

Chao, H., Wang, H., Wang, X., Guo, L., Gu, J., Zhao, W., et al. (2017). Genetic dissection of seed oil and protein content and identification of networks associated with oil content in *Brassica napus*. *Sci. Rep.* 7:46295. doi: 10.1038/srep46295

Chen, J., Liu, L., Wang, Z., Zhang, Y., Sun, H., Song, S., et al. (2020). Nitrogen fertilization increases root growth and coordinates the root–shoot relationship in cotton. *Front. Plant Sci.* 11:880. doi: 10.3389/fpls.2020.00880

Chin, S., Kwon, T., Khan, B. R., Alan Sparks, J., Mallery, E. L., Szymanski, D. B., et al. (2021). Spatial and temporal localization of SPIRRIG and WAVE/SCAR reveal roles for these proteins in actin-mediated root hair development. *Plant Cell* 33, 2131–2148. doi: 10.1093/plcell/koab115

Churchill, G. A., and Doerge, R. W. (1994). Empirical threshold values for quantitative trait mapping. *Genetics* 138, 963–971. doi: 10.1093/genetics/138.3.963

Coleto, I., Vega-Mas, I., Glauser, G., González-Moro, M. B., Marino, D., and Ariz, I. (2019). New insights on *Arabidopsis thaliana* root adaption to ammonium nutrition by the use of a quantitative proteomic approach. *Int. J. Mol. Sci.* 20:814. doi: 10.3390/ijms20040814

Colinas, M., and Fitzpatrick, T. B. (2016). Interaction between vitamin B6 metabolism, nitrogen metabolism and autoimmunity. *Plant Signal. Behav.* 11:e1161876. doi: 10.1080/15592324.2016.1161876

Collins, N. C. (2008). Quantitative trait loci and crop performance under abiotic stress: Where do we stand ? *Plant Physiol.* 147, 469–486. doi: 10.1104/pp.108.118117

Congreves, K. A., Otchere, O., Ferland, D., Farzadfar, S., Williams, S., and Arcand, M. M. (2021). Nitrogen use efficiency definitions of today and tomorrow. *Front. Mol. Biosci.* 12:637108. doi: 10.3389/fpls.2021.637108

Danakumara, T., Kumari, J., Singh, A. K., and Sinha, S. K. (2021). Genetic dissection of seedling root system architectural traits in a diverse panel of hexaploid wheat through multi-locus genome-wide association mapping for improving drought tolerance. *Int. J. Mol. Sci.* 22:7188. doi: 10.3390/ijms22197188

Das, D., Paries, M., Hobecker, K., Gigl, M., Dawid, C., Lam, H. M., et al. (2022). PHOSPHATE STARVATION RESPONSE transcription factors enable arbuscular mycorrhiza symbiosis. *Nat. Commun.* 13:477. doi: 10.1038/s41467-022-27976-8

Dong, X., and Duan, S. (2020). Plastid ribosomal protein LPE2 is involved in photosynthesis and the response to C/N balance in *Arabidopsis thaliana*. *J. Integr. Plant Biol.* 62, 1418–1432. doi: 10.1111/jipb.12907

Dormatey, R., Sun, C., Ali, K., Coulter, A., Bi, Z., and Bai, J. (2020). Gene pyramiding for sustainable crop improvement against biotic and abiotic stresses. *Agronomy* 10:1255.

Dun, X., Shi, J., Liu, H., Wang, J., Wang, X., and Wang, H. (2019). Genetic dissection of root morphological traits as related to potassium use efficiency in rapeseed under two contrasting potassium levels by hydroponics. *Sci. China Life Sci.* 62, 746–757. doi: 10.1007/s11427-018-9503-x

Ehrary, A., Rosas, M., Carpinelli, S., Davalos, O., Cowling, C., Fernandez, F., et al. (2020). Glutaredoxin *AtGRXS8* represses transcriptional and developmental responses to nitrate in *Arabidopsis thaliana* roots. *Plant Direct* 4:e00227. doi: 10.1002/pld3.227

Fan, X., Zhou, X., Chen, H., Tang, M., and Xie, X. (2021). Cross-talks between macro- and micronutrient uptake and signaling in plants. *Front. Plant Sci.* 12:663477. doi: 10.3389/fpls.2021.663477

Garcia, T., Duitama, J., Zullo, S. S., Gil, J., Dohle, S., Palkovic, A., et al. (2021). Comprehensive genomic resources related to domestication and crop improvement traits in Lima bean. *Nat. Commun.* 12:702. doi: 10.1038/s41467-021-20921-1

García-González, J., and van Gelderen, K. (2021). Bundling up the role of the actin cytoskeleton in primary root growth. *Front. Plant Sci.* 12:777119. doi: 10.3389/fpls.2021.777119

Goto, S., Mori, H., Uchiyama, K., Ishizuka, W., Taneda, H., Kono, M., et al. (2021). Genetic dissection of growth and eco-physiological traits associated with altitudinal adaptation in sakhalin fir (*Abies sachalinensis*) based on QTL mapping. *Genes* 12:1110. doi: 10.3390/genes12081110

Guo, Y., and Xu, F. K. Y. (2012). QTL mapping for seedling traits in wheat grown under varying concentrations of N, P and K nutrients. *Theor. Appl. Genet.* 124, 851–865. doi: 10.1007/s00122-011-1749-7

Hatfield, J. L., and Dold, C. (2019). Water-use efficiency: Advances and challenges in a changing climate. *Front. Plant Sci.* 10:103. doi: 10.3389/fpls.2019.00103

Hawkesford, M. J., and Griffiths, S. (2019). Exploiting genetic variation in nitrogen use efficiency for cereal crop improvement. *Curr. Opin. Plant Biol.* 49, 35–42. doi: 10.1016/j.pbi.2019.05.003

Hina, A., Cao, Y., Song, S., Li, S., Sharmin, R. A., Elattar, M. A., et al. (2020). High-resolution mapping in two RIL populations refines major "QTL Hotspot" regions for seed size and shape in soybean (*Glycine max* L.). *Int. J. Mol. Sci.* 21:1040. doi: 10.3390/ijms21031040

Hoagland, D. R., and Arnon, D. I. (1950). The water-culture method for growing plants without soil. *Circ. Calif. Agric. Exp. Stn.* 347:32.

Huo, L., Guo, Z., Zhang, Z., Jia, X., Sun, Y., Sun, X., et al. (2020). The apple autophagy-related gene *MdATG9* confers tolerance to low nitrogen in transgenic apple callus. *Front. Plant Sci.* 11:423. doi: 10.3389/fpls.2020.00423

Ibrahim, S., Li, K., Ahmad, N., Kuang, L., Sadau, S. B., Tian, Z., et al. (2021). Genetic dissection of mature root characteristics by genome-wide association studies in rapeseed (*Brassica napus* L.). *Plants* 10:2569. doi: 10.3390/PLANTS10122569

Islam, W., Tauqeer, A., Waheed, A., and Zeng, F. (2022). MicroRNA mediated plant responses to nutrient stress. *Int. J. Mol. Sci.* 23:2562.

Janes, G., von Wangenheim, D., Cowling, S., Kerr, I., Band, L., French, A. P., et al. (2018). Cellular patterning of *Arabidopsis* roots under low phosphate conditions. *Front. Plant Sci.* 9:735. doi: 10.3389/fpls.2018.00735

Jewel, Z. A., Ali, J., Mahender, A., Hernandez, J., Pang, Y., and Li, Z. (2019). Identification of quantitative trait loci associated with nutrient use efficiency traits, using SNP markers in an early backcross population of rice (*Oryza sativa* L.). *Int. J. Mol. Sci.* 20:900. doi: 10.3390/ijms20040900

Jiao, X., Lyu, Y., Wu, X., Li, H., Cheng, L., Zhang, C., et al. (2016). Grain production versus resource and environmental costs: Towards increasing sustainability of nutrient use in China. *J. Exp. Bot.* 67, 4935–4949. doi: 10.1093/jxb/erw282

Justamante, M. S., Ibáñez, S., Peidró, A., and Julkowska, M. M. (2019). A genome-wide association study identifies new loci involved in wound-induced lateral root formation in *Arabidopsis thaliana*. *Front. Plant Sci.* 10:311. doi: 10.3389/fpls.2019.00311

Kang, L., Qian, L., Zheng, M., Chen, L., Chen, H., Yang, L., et al. (2021). Genomic insights into the origin, domestication and diversification of *Brassica juncea*. *Nat. Genet.* 53, 1392–1402. doi: 10.1038/s41588-021-00922-y

Kim, M., Nguyen, T. T. P., Ahn, J. H., Kim, G. J., and Sim, S. C. (2021). Genome-wide association study identifies QTL for eight fruit traits in cultivated tomato (*Solanum lycopersicum* L.). *Hortic. Res.* 8:203. doi: 10.1038/s41438-021-00638-4

Kuang, L., Ahmad, N., Su, B., Huang, L., Li, K., Wang, H., et al. (2022). Discovery of genomic regions and candidate genes controlling root development using a recombinant inbred line population in rapeseed (*Brassica napus* L.). *Int. J. Mol. Sci.* 23:4781. doi: 10.3390/ijms23094781

Kuang, Q., Zhang, S., Wu, P., Chen, Y., and Li, M. (2017). Global gene expression analysis of the response of physic nut (*Jatropha curcas* L.) to medium- and long-term nitrogen deficiency. *PLoS One* 12:e0182700. doi: 10.1371/journal.pone.0182700

Larson, E. R., Domozych, D. S., and Tierney, M. L. (2014). SNARE VTI13 plays a unique role in endosomal trafficking pathways associated with the vacuole and is essential for cell wall organization and root hair growth in *Arabidopsis*. *Ann. Bot.* 114, 1147–1159. doi: 10.1093/aob/mcu041

Lee, Y. J., Lee, W. J., Le, Q. T., Hong, S., and Lee, H. (2021). Growth performance can be increased under high nitrate and high salt stress through enhanced nitrate

reductase activity in *Arabidopsis* anthocyanin over-producing mutant plants. *Front. Plant Sci.* 12:644455. doi: 10.3389/fpls.2021.644455

Lešková, A., Zvarík, M., Araya, T., and Giehl, R. F. H. (2020). Nickel toxicity targets cell wall-related processes and PIN2-mediated auxin transport to inhibit root elongation and gravitropic responses in *Arabidopsis. Plant Cell Physiol.* 61, 519–535. doi: 10.1093/pcp/pcz217

Li, K., Wang, J., Kuang, L., Tian, Z., Wang, X., Dun, X., et al. (2021). Genome-wide association study and transcriptome analysis reveal key genes affecting root growth dynamics in rapeseed. *Biotechnol. Biofuels* 14:178. doi: 10.1186/s13068-021-02032-7

Li, X., Sanagi, M., Lu, Y., Nomura, Y., Stolze, S. C., Yasuda, S., et al. (2020). Protein phosphorylation dynamics under carbon/nitrogen-nutrient stress and identification of a cell death-related receptor-like kinase in *Arabidopsis. Front. Plant Sci.* 11:377. doi: 10.3389/fpls.2020.00377

Li, Z., Mei, S., and Mei, Z. (2014). Mapping of QTL associated with waterlogging tolerance and drought resistance during the seedling stage in oilseed rape (*Brassica napus* L.). *Euphytica* 197, 341–353. doi: 10.1007/s10681-014-1070-z

Liu, Z., Gao, K., Shan, S., Gu, R., Wang, Z., and Craft, E. J. (2017). Comparative analysis of root traits and the associated QTLs for maize seedlings grown in paper roll, hydroponics and vermiculite culture system. *Front. Plant Sci.* 8:436. doi: 10.3389/fpls.2017.00436

Liu, Z., She, H., Xu, Z., Zhang, H., Li, G., Zhang, S., et al. (2021). Quantitative trait loci (QTL) analysis of leaf related traits in spinach (*Spinacia oleracea* L.). *BMC Plant Biol.* 21:290. doi: 10.1186/s12870-021-03092-5

Lu, K., Wei, L., Li, X., Wang, Y., Wu, J., Liu, M., et al. (2019). Whole-genome resequencing reveals *Brassica napus* origin and genetic loci involved in its improvement. *Nat. Commun.* 10:1154. doi: 10.1038/s41467-019-09134-9

Lynch, J. P. (2019). Tansley review root phenotypes for improved nutrient capture: An underexploited opportunity for global agriculture. *New Phytol.* 223, 548–564. doi: 10.1111/nph.15738

Ma, A., Huang, Z., Wang, X., Xu, Y., and Guo, X. (2021). Identification of quantitative trait loci associated with upper temperature tolerance in turbot, *Scophthalmus maximus. Sci. Rep.* 11:21920. doi: 10.1038/s41598-021-01062-3

Marzol, E., Borassi, C., Sardoy, M. C., Ranocha, P., Aptekmann, A. A., Bringas, M., et al. (2022). Class III peroxidases PRX01, PRX44, and PRX73 control root hair growth in *Arabidopsis thaliana. Int. J. Mol. Sci.* 23:5375. doi: 10.3390/ijms23105375

Mase, K., and Tsukagoshi, H. (2021). Reactive oxygen species link gene regulatory networks during *Arabidopsis* root development. *Front. Plant Sci.* 12:660274. doi: 10.3389/fpls.2021.660274

McGrail, R. K., Van Sanford, D. A., and McNear, D. H. (2020). Trait-based root phenotyping as a necessary tool for crop selection and improvement. *Agronomy* 10:1328.

Mei, J., Shao, C., Yang, R., Feng, Y., Gao, Y., Ding, Y., et al. (2020). Introgression and pyramiding of genetic loci from wild *Brassica oleracea* into *B.napus* for improving *Sclerotinia* resistance of rapeseed. *Theor. Appl. Genet.* 133, 1313–1319. doi: 10.1007/s00122-020-03552-w

Mensah, S. T., Ochekwu, E. B., Mgbedo, U. G., and Uzoma, M. C. (2020). Effect of N: P: K (15: 15: 15) on the growth of *Punica granatum* L. seedlings. *Int. J. Agron.* 2020:4653657. doi: 10.1155/2020/4653657

Peltier, E., Bibi-triki, S., Dutreux, F., Caradec, C., Friedrich, A., and Llorente, B. (2021). Dissection of quantitative trait loci in the *Lachancea waltii* yeast species highlights major hotspots. *G3* 11:jkab247. doi: 10.1093/g3journal/jkab242

Podg, A., Id, M. O., Borysiuk, K., Tarnowska, A., Jakubiak, M., Burian, M., et al. (2018). Suppression of external NADPH dehydrogenase — NDB1 in *Arabidopsis thaliana* confers improved tolerance to ammonium toxicity via efficient glutathione/redox metabolism. *Int. J. Mol. Sci.* 19:1412. doi: 10.3390/ijms19051412

Prakash, P. T., Banan, D., Paul, R. E., Feldman, M. J., Xie, D., Freyfogle, L., et al. (2021). Correlation and co-localization of QTL for stomatal density, canopy temperature, and productivity with and without drought stress in *Setaria. J. Exp. Bot.* 72, 5024–5037. doi: 10.1093/jxb/erab166

Rao, V. S., Srinivas, K., Sujini, G. N., and Kumar, G. N. S. (2014). Protein-protein interaction detection: Methods and analysis. *Int. J. Proteomics* 2014:147648. doi: 10.1155/2014/147648

Rath, M., Dümmer, M., Galland, P., and Forreiter, C. (2020). ORIGINAL RESEARCH: A gravitropic stimulus alters the distribution of EHB1, a negative effector of root gravitropism in *Arabidopsis. Plant Direct* 4:e00215. doi: 10.1002/pld3.215

Ren, Y., Qian, Y., Xu, Y., Zou, C., and Liu, D. (2017). Characterization of QTLs for root traits of wheat grown under different nitrogen and phosphorus supply levels. *Front. Plant Sci.* 8:2096. doi: 10.3389/fpls.2017.02096

Rossdeutsch, L., Schreiner, R. P., Skinkis, P. A., and Deluc, L. (2021). Nitrate uptake and transport properties of two grapevine rootstocks with varying vigor. *Front. Plant Sci.* 11:608813. doi: 10.3389/fpls.2020.608813

Rotmistrovsky, K., Jang, W., and Schuler, G. D. (2004). A web server for performing electronic PCR. *Nucleic Acids Res.* 32, 108–112. doi: 10.1093/nar/gkh450

Roy, J., Shaikh, T. M., Mendoza, R., Hosain, S., and Chapara, V. (2021). Genome-wide association mapping and genomic prediction for adult stage sclerotinia stem rot resistance in *Brassica napus* L. under field environments. *Sci. Rep.* 11:21773. doi: 10.1038/s41598-021-01272-9

Sahito, J. H., Zhang, X., Zhong, H., He, X., Zhen, C., Ma, P., et al. (2020). Identification, association of natural variation and expression analysis of *ZmNAC9* gene response to low phosphorus in maize seedling stage. *Plants* 9:1447. doi: 10.3390/plants9111447

Samuilov, S., Brilhaus, D., Rademacher, N., Flachbart, S., Arab, L., Alfarraj, S., et al. (2018). The photorespiratory BOU gene mutation alters sulfur assimilation and its crosstalk with carbon and nitrogen metabolism in *Arabidopsis thaliana. Front. Plant Sci.* 871:1709. doi: 10.3389/fpls.2018.01709

Sandhu, N., Kaur, A., Sethi, M., and Kaur, S. (2021). Genetic dissection uncovers associations for plant growth, yield, and yield-related traits under varying nitrogen levels in nested synthetic wheat introgression libraries. *Front. Plant Sci.* 12:738710. doi: 10.3389/fpls.2021.738710

Shen, X., Yuan, Y., Zhang, H., Guo, Y., Zhao, Y., Li, S., et al. (2019). The hot QTL locations for potassium, calcium, and magnesium nutrition and agronomic traits at seedling and maturity stages of wheat under different potassium treatments. *Genes* 10:607. doi: 10.3390/genes10080607

Soriano, J. M., Colasuonno, P., Marcotuli, I., and Gadaleta, A. (2021). Meta-QTL analysis and identification of candidate genes for quality, abiotic and biotic stress in durum wheat. *Sci. Rep.* 11:11877. doi: 10.1038/s41598-021-91446-2

Stahl, A., Vollrath, P., Samans, B., Frisch, M., Wittkop, B., and Snowdon, R. J. (2019). Effect of breeding on nitrogen use efficiency-associated traits in oilseed rape. *J. Exp. Bot.* 70, 1969–1986. doi: 10.1093/jxb/erz044

Stoll, M., Kwitek-black, A. E., Cowley, A. W., Harris, E. L., Harrap, S. B., Krieger, E., et al. (2000). New target regions for human hypertension via comparative genomics. *Genome Res.* 10, 473–482.

Sun, X., Ren, W., Wang, P., Chen, F., Yuan, L., Pan, Q., et al. (2021). Evaluation of maize root growth and genome-wide association studies of root traits in response to low nitrogen supply at seedling emergence. *Crop J.* 9, 794–804. doi: 10.1016/j.cj.2020.09.011

Szklarczyk, D., Gable, A. L., Nastou, K. C., Lyon, D., Kirsch, R., Pyysalo, S., et al. (2021). The STRING database in 2021: Customizable protein-protein networks, and functional characterization of user-uploaded gene/measurement sets. *Nucleic Acids Res.* 49, D605–D612. doi: 10.1093/nar/gkaa1074

Thorup-Kristensen, K., and Kirkegaard, J. (2016). Root system-based limits to agricultural productivity and efficiency: The farming systems context. *Ann. Bot.* 118, 573–592. doi: 10.1093/aob/mcw122

Tian, Z., Li, Y., Liang, Z., Guo, H., Cai, J., Jiang, D., et al. (2016). Genetic improvement of nitrogen uptake and utilization of winter. *Field Crops Res.* 196, 251–260. doi: 10.1016/j.fcr.2016.07.007

Trujillo-Hernandez, J. A., Bariat, L., Enders, T. A., and Strader, L. C. (2020). RESEARCH PAPER: A glutathione-dependent control of the indole butyric acid pathway supports *Arabidopsis* root system adaptation to phosphate deprivation. *J. Exp. Bot.* 71, 4843–4857. doi: 10.1093/jxb/eraa195

Vega, A., Fredes, I., O'Brien, J., Shen, Z., Ötvös, K., Abualia, R., et al. (2021). Nitrate triggered phosphoproteome changes and a PIN2 phosphosite modulating root system architecture. *EMBO Rep.* 22:e51813. doi: 10.15252/embr.20205 1813

Velinov, V., Vaseva, I., Zehirov, G., Zhiponova, M., Georgieva, M., Vangheluwe, N., et al. (2020). Overexpression of the *NMig1* gene encoding a NudC domain protein enhances root growth and abiotic stress tolerance in *Arabidopsis thaliana. Front. Plant Sci.* 11:815. doi: 10.3389/fpls.2020.00815

Vijayakumar, P., Datta, S., and Dolan, L. (2016). ROOT HAIR DEFECTIVE SIX-LIKE4 (RSL4) promotes root hair elongation by transcriptionally regulating the expression of genes required for cell growth. *New Phytol.* 212, 944–953. doi: 10.1111/nph.14095

Wang, J., Dun, X., Shi, J., Wang, X., Liu, G., and Wang, H. (2017). Genetic dissection of root morphological traits related to nitrogen use efficiency in *Brassica napus* L. Under two contrasting nitrogen conditions. *Front. Plant Sci.* 8:1709. doi: 10.3389/fpls.2017.01709

Wang, J., Lan, P., Gao, H., Zheng, L., Li, W., and Schmidt, W. (2013). Expression changes of ribosomal proteins in phosphate- and iron-deficient *Arabidopsis* roots

predict stress-specific alterations in ribosome composition. *BMC Genomics* 14:783. doi: 10.1186/1471-2164-14-783

Wang, L., Xu, Q., Yu, H., Li, X., Yang, J., Chu, J., et al. (2020). Strigolactone and karrikin signaling pathways elicit ubiquitination and proteolysis of SMXL2 to regulate. *Plant Cell* 32, 2251–2270. doi: 10.1105/tpc.20.00140

Wang, W., Ding, G., and White, P. J. (2019). Mapping and cloning of quantitative trait loci for phosphorus efficiency in crops: Opportunities and challenges. *Plant Soil* 439, 91–112. doi: 10.1007/s11104-018-3706-6

Wang, X., Chen, L., Wang, A., Wang, H., Tian, J., Zhao, X., et al. (2016). Quantitative trait loci analysis and genome-wide comparison for silique related traits in *Brassica napus*. *BMC Plant Biol.* 16:71. doi: 10.1186/s12870-016-0759-7

Wang, Z., Chen, Z., Cheng, J., Lai, Y., Wang, J., Bao, Y., et al. (2012a). QTL analysis of Na$^+$ and K$^+$ concentrations in roots and shoots under different levels of NaCl stress in rice (*Oryza sativa* L.). *PLoS One* 7:e51202. doi: 10.1371/journal.pone.0051202

Wang, S., Basten, C. J., and Zeng, Z. (2012b). *Windows QTL cartographer 2.5*. Raleigh, NC: Department of Statistics, North Carolina State University.

Wissuwa, M., Kretzschmar, T., and Rose, T. J. (2016). From promise to application: Root traits for enhanced nutrient capture in rice breeding. *J. Exp. Bot.* 67, 3605–3615. doi: 10.1093/jxb/erw061

Woo, J., MacPherson, C. R., Liu, J., Wang, H., Kiba, T., Hannah, M. A., et al. (2012). The response and recovery of the *Arabidopsis thaliana* transcriptome to phosphate starvation. *BMC Plant Biol.* 12:62. doi: 10.1186/1471-2229-12-62

Wu, Y., Chang, Y., Luo, L., Tian, W., Gong, Q., and Liu, X. (2022). Abscisic acid employs NRP-dependent PIN2 vacuolar degradation to suppress auxin-mediated primary root elongation in *Arabidopsis*. *New Phytol.* 233, 297–312. doi: 10.1111/nph.17783

Xu, P., and Cai, W. (2019). Nitrate-responsive OBP4-XTH9 regulatory module controls lateral root development in *Arabidopsis thaliana*. *PLoS Genet.* 15:e1008465. doi: 10.1371/journal.pgen.1008465

Xun, Q., and Gou, X. (2020). Two receptor-like protein kinases, MUSTACHES and MUSTACHES-LIKE, regulate lateral root development in *Arabidopsis thaliana*. *New Phytol.* 227, 1157–1173. doi: 10.1111/nph.16599

Yang, Z., Xu, J., Du, L., Yin, J., Wang, Z., Yi, F., et al. (2022). Design, synthesis, and action mechanism of 1, 3-benzodioxole derivatives as potent auxin receptor agonists and root growth promoters virtual screening and artificial synthesis. *Front. Plant Sci.* 13:902902. doi: 10.3389/fpls.2022.902902

Zeng, Y., Verstraeten, I., Trinh, H. K., Heugebaert, T., Stevens, C. V., Garcia-Maquilon, I., et al. (2021). Arabidopsis hypocotyl adventitious root formation is suppressed by ABA signaling. *Genes* 12:1141. doi: 10.3390/genes12081141

Zhao, L., Zhang, W., Yang, Y., Li, Z., Li, N., Qi, S., et al. (2018). The *Arabidopsis* NLP7 gene regulates nitrate signaling via NRT1.1-dependent pathway in the presence of ammonium. *Sci. Rep.* 8:1487. doi: 10.1038/s41598-018-20038-4

Zhen, X., Id, F. X., Zhang, W., Li, N., and Li, X. (2019). Overexpression of rice gene *OsATG8b* confers tolerance to nitrogen starvation and increases yield and nitrogen use efficiency (NUE) in *Arabidopsis*. *PLoS One* 14:e0223011. doi: 10.1371/journal.pone.0223011